

Synthesis and structure of stable base-free dialkylsilanimines†‡

Takeaki Iwamoto,*^a Nobuyoshi Ohnishi,^a Zhenyu Gui,^a Shintaro Ishida,^a
Hiroyuki Isobe,^a Satoshi Maeda,^b Koichi Ohno^b and Mitsuo Kira*^a

Received (in Montpellier, France) 15th February 2010, Accepted 18th March 2010

DOI: 10.1039/c0nj00121j

Four isolable dialkylsilanimines $R^H_2Si=NR$ ($R = CH_2Ph$ (**5a**), Ph (**5b**), 1-adamantyl (**5c**) and $SiMe_3$ (**5d**), where $R^H_2 = 1,1,4,4$ -tetrakis(trimethylsilyl)butane-1,4-diyl) were synthesized as air-sensitive crystals by the reaction of isolable dialkylsilylene **4** with the corresponding azides. X-ray analysis shows that **5a–5d** are base-free silanimines and **5a** and **5b** have a remarkable bent $Si=N-R$ structure, while **5c** and **5d** have an almost linear structure. Distinct $\pi(Si=N) \rightarrow \pi^*(Si=N)$ and $n(N) \rightarrow \pi^*(Si=N)$ transition bands of silicon–nitrogen double bonds were observed for **5a–5d** in hexane. A mechanism for the formation of silanimine from the reaction of silylene and azide is discussed using theoretical calculations with the GRRM method for model reactions.

Introduction

Since the first synthesis of stable silenes ($R_2Si=CR_2$) by Brook¹ and of disilenes ($R_2Si=SiR_2$) by West,² various stable unsaturated silicon compounds have been synthesized using kinetic and/or electronic stabilization, and the chemistry of stable unsaturated silicon compounds has become one of the most exciting fields of organosilicon chemistry.³

Silanimines ($R_2Si=NR'$) are fascinating compounds because they are silicon analogs of imines, which are important functional groups in organic chemistry. Wiberg *et al.* synthesized the first stable silanimine ($t-Bu$)₂Si=NSi($t-Bu$)₃ (**1**), and isolated it as the THF-coordinated form in 1985⁴ and the THF-free form in 1986.⁵ Klingebiel *et al.* then showed that base-free ($i-Pr$)₂Si=N(2,4,6- $i-Pr$)₃C₆H₂ (**2**) can be isolated as orange crystals in 1986.⁶ Since then, several stable silanimines have been investigated.^{7–9} Nevertheless, most stable silanimines are stabilized by the coordination to the Si=N moiety, for instance, with Lewis bases⁷ or alkali metal halides⁸ ligated to the unsaturated silicon atoms, and transition metals ligated to the unsaturated bond.⁹ *N*-Silylated silanimines **1**⁵ and ($t-Bu$)₂Si=NSi($t-Bu$)₂Ph (**3**)¹⁰ are the only examples of base-free silanimines whose structure was determined by X-ray crystallography. Therefore, synthesis and chemical properties of stable base-free silanimines that should show the intrinsic structures and properties of the silicon–nitrogen double bond still remain to be elucidated.

Recently, we have applied isolable dialkylsilylene **4** (R^H_2Si ; $R^H_2 = 1,1,4,4$ -tetrakis(trimethylsilyl)butane-1,4-diyl),¹¹ to the synthesis of various types of stable unsaturated silicon compounds such as trisilaallene,^{12a} 2-germadisilaallene,^{12b} silanechalcogenones,^{12c} fused tricyclic disilenes,^{12d} silaketenimines^{12e} and tetrasiladienes,^{12f} and demonstrated that silylene **4** is a useful building block for synthesis of stable unsaturated silicon compounds. In the present paper, we would like to report the synthesis and properties of base-free dialkylsilanimines **5** ($R^H_2Si=NR$) with a series of substituents on the nitrogen atom. X-ray analysis shows an interesting substituent effect of silanimines **5** on the bending of the Si=N-R moiety. Distinct $\pi(Si=N) \rightarrow \pi^*(Si=N)$ and $n(N) \rightarrow \pi^*(Si=N)$ transition bands were observed in the UV-vis spectra. A mechanism for the formation of silanimines from the corresponding silylene and azides is proposed using theoretical calculations for model reactions from the global reaction route mapping (GRRM) method (by Ohno and Maeda),¹³ which enables automated and systematic reaction global mapping on the potential energy surface of a given chemical formula.

Results and discussion

Synthesis of dialkylsilanimines

Dialkylsilanimines **5a–5d** can be synthesized by the reactions of dialkylsilylene **4** with the corresponding azides.^{7e,14} Typically, to a hexane solution of **4**, one equivalent of (azidomethyl)-benzene in hexane was added dropwise at room temperature (eqn (1)).¹⁵ The color of the solution immediately turned from orange to pale yellow with evolution of gas. After stirring the mixture for 5 min at room temperature, the volatiles were removed *in vacuo*. Recrystallization from hexane gave analytically pure air-sensitive colorless crystals of (*N*-benzyl)-silanimine **5a** in 86% yield. Silanimines **5b** ($R = Ph$; pale yellow crystals, 77%), **5c** ($R = 1$ -adamantyl; colorless crystals, 88%) and **5d** ($R = SiMe_3$; colorless crystals, 82%) were synthesized (eqn (1)) in a similar manner. The molecular structures of silanimines **5a–5d** were determined by ¹H, ¹³C

^a Department of Chemistry, Graduate School of Science, Tohoku University, Aoba-ku, Sendai 980-8578, Japan.
E-mail: iwamoto@m.tains.tohoku.ac.jp;

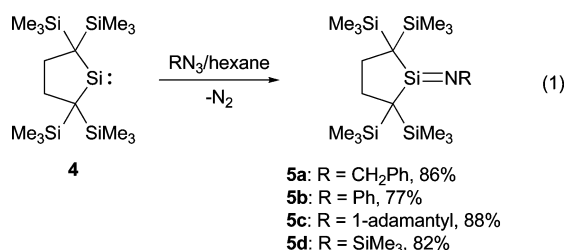
Fax: +81 22 795 7714; Tel: +81 22 795 7714

^b Toyota Physical and Chemical Research Institute, Nagakute, Aichi 480-1192, Japan

† Electronic supplementary information (ESI) available: Details of theoretical study. CCDC reference numbers 766385–766388. For ESI and crystallographic data in CIF or other electronic format see DOI: 10.1039/c0nj00121j

‡ This article is part of a themed issue on Main Group Chemistry, and is dedicated to the late Prof. Pascal Le Floch (*NJC* co-Editor-in-Chief, deceased March 2010) in honour of his remarkable contributions to main group chemistry.

and ^{29}Si NMR spectroscopy, MS spectrometry, elemental analysis and X-ray crystallography.



Silylene **4** reacted with the azide in a 1 : 1 manner to give the corresponding silanimines **5**, even when we varied the stoichiometry of the reagents: when either excess silylene **4** or the azide was used, the corresponding silanimine was obtained along with the recovery of the excess starting materials (**4** or azides). In contrast, West *et al.* and Lappert *et al.* have reported that, when a *N*-heterocyclic silylene reacted with an excess amount of the azide, the 1:2 adduct (such as tetraazasiloranes or azidoaminosilanes) was obtained,^{16b,d} and when an excess amount of *N*-heterocyclic silylene reacted with the azide, the 2:1 adduct (diazasilacyclopropanes) was obtained.^{7e,16} Severe steric hindrance of silylene **4** may prevent further addition of **4** or the azides to the resulting silanimines **5**.

Molecular structures of silanimines **5a–5d**

Single crystals of silanimines **5a–5d** suitable for X-ray single crystal analysis were obtained by recrystallization from hexane. The molecular structures of **5a–5d** determined by X-ray analysis are displayed in Fig. 1–4 and the selected structural parameters of **5a–5d** and related silanimines are summarized in Table 1. Compound **5** is the first example of a base-free silanimine with a carbon functional-group on the nitrogen atom.

X-ray analysis shows that silanimines **5a–5d** have base-free silicon–nitrogen double bonds. Thus, silanimines **5a–5d** have planar tricoordinated unsaturated silicon atoms with the sum of bond angles around the silicon atom ($\Sigma \varphi(\text{Si})$) of 360°, similar to base-free silanimines **1**⁵ and **3**.¹⁰ The silicon–nitrogen distances in **5a–5d** (1.5496(14)–1.5858(9) Å) are much shorter than the range of silicon–nitrogen single-bond distances (1.65–1.85 Å)¹⁷ and close to those of **1** (1.568(3) Å) and **3** (1.573(2) Å). To the best of our knowledge, the Si=N distance of silanimine **5c** is the shortest (1.5496(14) Å) among the hitherto known silanimines.

The most striking structural feature was found in the geometry around the nitrogen atom. Although silanimines **5c** and **5d** have an almost linear structure with Si–N–R bending angles θ of 173.30(15)° and 177.19(13)°, respectively, similarly to base-free *N*-silylated silanimine **1** ($\theta = 177.8(2)^\circ$)⁵ and **3** ($\theta = 168.34(16)^\circ$),¹⁰ **5a** and **5b** adopt a remarkably bent structure with θ of 138.07(15) and 144.42(8)°. Since theoretical calculations have predicted that silanimines have quite flat potential surfaces with respect to the inversion in plane (for instance, the inversion barrier of the bent silanimine H₂Si=NH with angle θ of 126.6° are predicted to be only 25.1 kJ mol⁻¹ at the MP4/6-31G(d) level),¹⁸ both electronic and steric effects on *N*-substituents of **5a–5d** could be

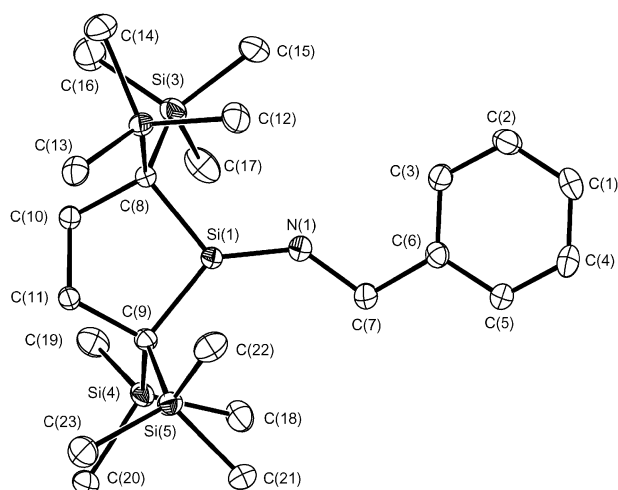


Fig. 1 ORTEP drawing of silanimine **5a**. Hydrogen atoms are omitted for clarity. Thermal ellipsoids are shown at the 50% probability level. Selected bond lengths (Å) and angles (°): Si(1)–N(1) 1.5823(18), Si(1)–C(8) 1.863(2), Si(1)–C(9) 1.871(2), N(1)–C(7) 1.446(3), Si(1)–N(1)–C(7) 138.07(15), N(1)–Si(1)–C(8) 123.13(9), N(1)–Si(1)–C(9) 134.84(9), C(8)–Si(1)–C(9) 102.02(9), Si(1)–N(1)–C(7)–C(6) –161.39(19), N(1)–C(7)–C(6)–C(3) –7.8(3).

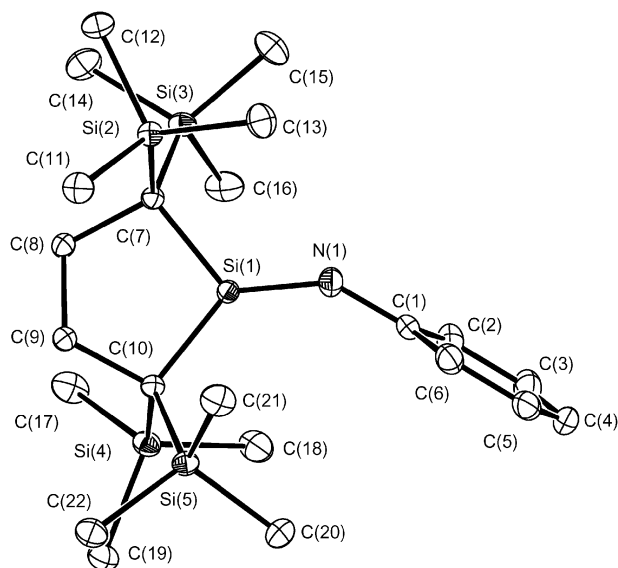


Fig. 2 ORTEP drawing of silanimine **5b**. Hydrogen atoms are omitted for clarity. Thermal ellipsoids are shown at the 50% probability level. Selected bond lengths (Å) and angles (°): Si(1)–N(1) 1.5858(9), Si(1)–C(7) 1.8477(10), Si(1)–C(10) 1.8618(11), Si(1)–N(1)–C(1) 144.42(8), C(7)–Si(1)–N(1) 123.60(5), C(10)–Si(1)–N(1) 133.79(5), C(7)–Si(1)–C(10) 102.61(5), Si(1)–N(1)–C(1)–C(2) 93.83(16).

responsible for the geometry around the Si=N double bond. However, the nearly linear Si=N–R geometry of *N*-silyl-silanimine **5d** would be mainly owing to the electronic rather than steric effect of the silyl substituents, because similar linear geometries have been observed in *N*-silylsilanimines **1** and **3** and well reproduced by the calculation of a model compound H₂Si=N–SiH₃ ($\theta = 175.6^\circ$ at the MP4/6-31G(d) level).¹⁸ Similar substituent dependence of the geometry around the

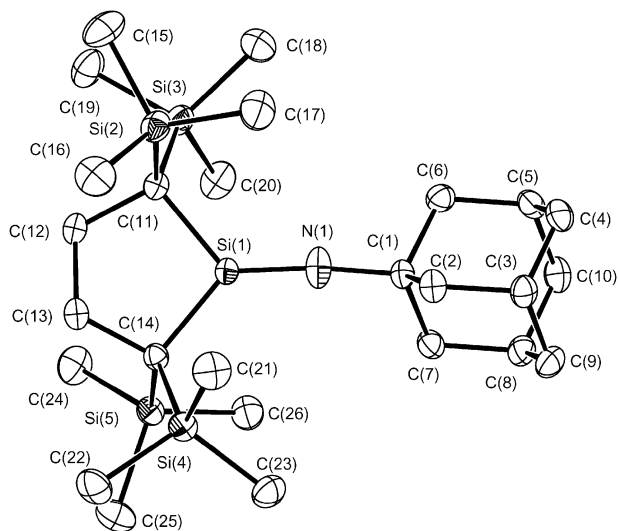


Fig. 3 ORTEP drawing of silanimine **5c**. Hydrogen atoms are omitted for clarity. Thermal ellipsoids are shown at the 50% probability level. Selected bond lengths (Å) and angles (°): Si(1)–N(1) 1.5496(14), Si(1)–C(11) 1.8751(16), Si(1)–C(14) 1.8766(16), N(1)–C(1) 1.426(2), Si(1)–N(1)–C(1) 173.30(15), C(11)–Si(1)–N(1) 127.30(8), C(14)–Si(1)–N(1) 131.72(8), C(11)–Si(1)–C(14) 100.98(7).

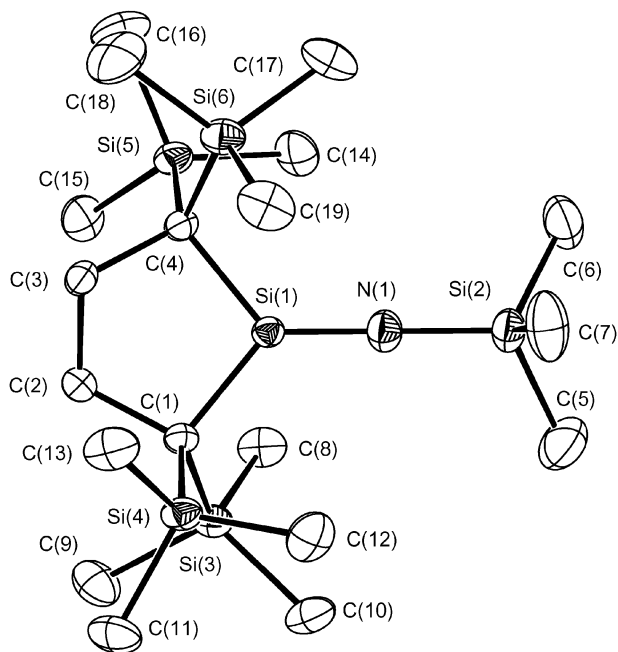


Fig. 4 ORTEP drawing of silanimine **5d**. Hydrogen atoms are omitted for clarity. Thermal ellipsoids are shown at the 50% probability level. Selected bond lengths (Å) and angles (°): Si(1)–N(1) 1.5685(18), N(1)–Si(2) 1.6762(19), Si(1)–C(1) 1.8554(19), Si(1)–C(4) 1.8573(19), Si(1)–N(1)–Si(2) 177.19(13), C(1)–Si(1)–N(1) 129.72(9), C(4)–Si(1)–N(1) 128.69(8), C(1)–Si(1)–C(4) 101.59(9).

carbon–nitrogen double bond have been observed in diphenyl-imines; the bent angle θ of *N*-silylated imine $\text{Ph}_2\text{C}=\text{NSi}^t\text{Bu}_3$ is $154.6(3)^\circ$,¹⁹ while those of *N*-carbon-substituted imines are 120.64° for $\text{Ph}_2\text{C}=\text{NPh}$ ²⁰ and $120.8(2)^\circ$ for $\text{Ph}_2\text{C}=\text{NCH}(\text{Ph})_2$.²¹ The Si=N double bond distances of bent

Table 1 Selected structural parameters of silanimines **5a–5d** and related base-free silanimines

Silanimine	$d(\text{Si}=\text{N})/\text{\AA}$	$\theta(\text{Si}-\text{N}-\text{R})/^\circ$	$\Sigma \varphi(\text{Si})^a$
5a (R = CH ₂ Ph)	1.5823(18)	138.07(15)	359.9(1)
5b (R = Ph)	1.5858(9)	144.42(8)	360.00(5)
5c (R = 1-Ad)	1.5496(14)	173.30(15)	360.00(8)
5d (R = SiMe ₃)	1.5685(18)	177.19(13)	360.00(8)
<i>t</i> -Bu ₂ Si=N ₂ Si(<i>t</i> -Bu) ₃ ^b	1.568(3)	177.8(2)	359.9(2)
<i>t</i> -Bu ₂ Si=N ₂ Si(<i>t</i> -Bu) ₂ Ph ^c	1.573(2)	168.34(16)	359.83(13)

^a Sum of the bond angles around the unsaturated silicon atom. ^b Ref. 5. ^c Ref. 10.

silanimines **5a** and **5b** (1.582(2) and 1.5858(9) Å) are slightly longer than those of linear silanimines **5c** and **5d** (1.5496(14) and 1.5685(18) Å). The relatively long Si=N distances in **5c** and **5d** compared with those of **5a** and **5b** would be ascribed to the high p-character of silanimine nitrogen orbitals owing to the remarkable bent geometry. The structural characteristics of silanimines **5a–5d** will be discussed in detail using DFT calculations (*vide infra*).

The phenyl ring plane in *N*-benzylsilanimine **5a** is roughly parallel to the π plane of the Si=N bond with a dihedral angle between mean plane C(8)–C(9)–Si(1)–N(1) and the mean plane of the phenyl ring of 15.68° . On the other hand, the phenyl ring in *N*-phenylsilanimine **5b** is almost perpendicular to the Si=N bond, with a dihedral angle Si(1)–N(1)–C(1)–C(2) of $93.83(16)^\circ$, probably because of severe steric interaction between the phenyl ring and the bulky trimethylsilyl substituents on the silacyclopentane ring, allowing the conjugation between n orbital of the silanimine nitrogen atom and π orbitals of the phenyl ring. Similar perpendicular geometries between $\pi(\text{silicon})$ and $\pi(\text{aromatic})$ systems was observed in stable disilenes with polycyclic aromatic substituents and the dialkylsilylene unit (**4**).^{12g}

In contrast to the molecular structure in the solid state, the ¹H NMR spectra of silanimines **5a–5d** in benzene-*d*₆ exhibit similar highly symmetric structures: thirty-six ¹H, twelve ¹³C, and four ²⁹Si nuclei in four trimethylsilyl groups and four ¹H and two ¹³C in two methylene groups in silacyclopentane ring are all equivalent, respectively. This suggests that silanimines **5a–5d** adopt a linear averaged structure in solution or a bent structure with very low inversion barrier of the Si=N–R moiety. The ²⁹Si resonances of unsaturated silicon atoms (δSi_u) appeared in the low-field region at 75.34 (**5a**), 59.1 (**5b**), 19.9 (**5c**) and 89.9 (**5d**). Interestingly, the δSi_u of **5c** appears at a rather higher field of 19.9 ppm compared with those of the other silanimines with a carbon functional-group on the nitrogen atom (**5a** and **5b**). Although the reason for the high-field shift remains unclear, the linear geometry around the nitrogen atom of **5c** may be responsible. The δSi_u of bent Me₂SiNMe (**6b**) with $\theta = 135^\circ$ is calculated to appear at +74.3 ppm using calculations at the GIAO/B3LYP/6-311+G(2df,p) level, while that of linear **6b** with $\theta = 180^\circ$ is calculated to appear at the higher field of –17.5 ppm.²²

UV-vis spectra of dialkylsilanimines

Very few studies have previously been devoted to the investigation of the electronic structure of silanimines.

Studies of transient silanimines $\text{Me}_3\text{Si}(\text{N}_3)\text{Si}=\text{NSiMe}_3$,²³ $\text{Mes}_2\text{Si}=\text{NMes}$ (Mes = 2,4,6-trimethylphenyl),²⁴ twisted bridgehead silanimines,²⁵ $\text{Ph}_2\text{Si}=\text{NPh}$ ²⁶ and $\text{Mes}_2\text{Si}=\text{NSiMe}_3$ ²⁷ in low-temperature matrices have shown that these silanimines exhibit an intense $\pi(\text{Si}=\text{N}) \rightarrow \pi^*(\text{Si}=\text{N})$ transition band at shorter wavelength and a weak $n(\text{N}) \rightarrow \pi^*(\text{Si}=\text{N})$ transition band at longer wavelength.

UV-vis absorption spectra and major absorption bands of silanimine **5a–5d** in hexane are summarized in Fig. 5–8 and Table 2, respectively. Dialkylsilanimines **5a**, **5c** and **5d** show two similar absorption bands, I and II. Band I, with a large extinction coefficient, is observed at 255, 246 and 245 nm for **5a**, **5c** and **5d**, while band II, with a small extinction coefficient, is observed at 315 (as a shoulder), 320 and 306 nm, respectively. According to the assignment of absorption bands of the transient silanimines, bands I and II are assignable to the $\pi(\text{Si}=\text{N}) \rightarrow \pi^*(\text{Si}=\text{N})$ and $n(\text{N}) \rightarrow \pi^*(\text{Si}=\text{N})$ transitions, respectively. In the case of *N*-phenylsilanimine **5b**, a medium absorption band III is observed at 289 nm (sh), together with bands I and II at 251 and 345 nm, similarly to transient $\text{Ph}_2\text{Si}=\text{NPh}$ ²⁶ (which shows three bands at 404, 292 and 241 nm). The nature of the bands I–III will be discussed in detail using TD-DFT calculations (*vide infra*).

Theoretical calculations

(1) Molecular structure. To understand the characteristics of the geometry around the $\text{Si}=\text{N}$ double bond in dialkylsilanimines **5a–5d**, DFT calculations of model compounds $\text{Me}_2\text{Si}=\text{NR}$ (R = SiH_3 (**6a**), CH_3 (**6b**), H (**6c**), F (**6d**)) were performed. Selected structural parameters of **6a–6d** optimized at the B3LYP/6-311+G(d,p) level are summarized in Table 3. All silanimines **6a–6d** are calculated to have planar tricoordinated silicon atoms, with a sum of bond angles around the unsaturated silicon atom of 360° . The bending angle θ of the silanimines are significantly dependent on the substituent on the nitrogen atom, as predicted for $\text{H}_2\text{Si}=\text{NR}$ (R = H and SiH_3) by Schleyer.^{18,28} *N*-Silyldimethylsilanimine **6a** adopts an almost linear geometry, with a bending angle θ of 173.83° and silicon–nitrogen distance $d(\text{Si}=\text{N})$ of 1.579 Å, similar to those for $\text{H}_2\text{Si}=\text{N}-\text{SiH}_3$ ($\theta = 175.6^\circ$ and $d(\text{Si}=\text{N}) = 1.549$ Å). It should be noted that θ decreases in the order **6a** (173.83°), **6b** (135.90°), **6c** (120.35°), **6d** (110.52°), while distance $d(\text{Si}=\text{N})$

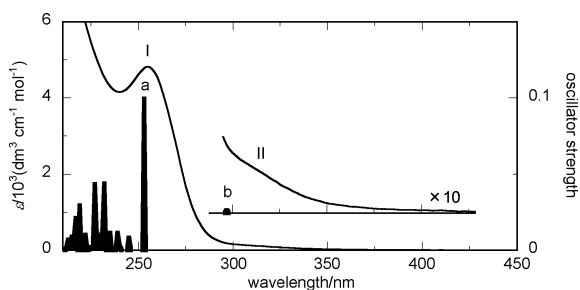


Fig. 5 UV-vis absorption spectrum of silanimine **5a** in hexane at room temperature superimposed with band positions calculated at the TD-B3LYP/6-311+G(d,p) level. Selected calculated transitions: a. $\pi(\text{Si}=\text{N}) \rightarrow \pi^*(\text{Si}=\text{N})$ transition. b. $n(\text{N}) \rightarrow \pi^*(\text{Si}=\text{N})$ transition.

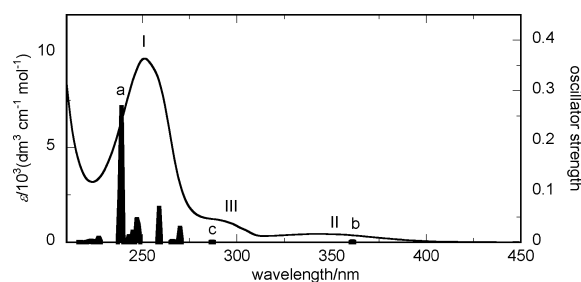


Fig. 6 UV-vis absorption spectrum of silanimine **5b** in hexane at room temperature superimposed with band positions calculated at the TD-B3LYP/6-311+G(d,p) level. Selected calculated transitions: a. $\pi(\text{Si}=\text{N}) \rightarrow \pi^*(\text{Si}=\text{N})$ transition. b. $n(\text{N}) \rightarrow \pi^*(\text{Si}=\text{N})$ transition. c. $\pi(\text{phenyl}) \rightarrow \pi^*(\text{Si}=\text{N})$ transition.

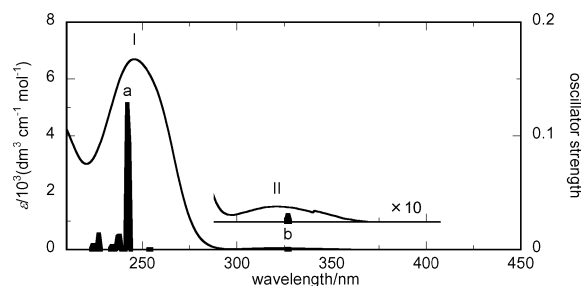


Fig. 7 UV-vis absorption spectrum of silanimine **5c** in hexane at room temperature superimposed with band positions calculated at the TD-B3LYP/6-311+G(d,p) level. Selected calculated transitions: a. assignable to $\pi(\text{Si}=\text{N}) \rightarrow \pi^*(\text{Si}=\text{N})$ transition. b. assignable to $n(\text{N}) \rightarrow \pi^*(\text{Si}=\text{N})$ transition.

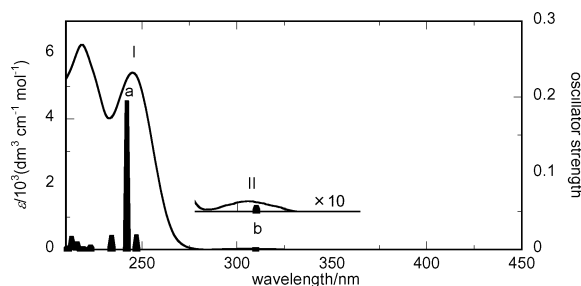


Fig. 8 UV-vis absorption spectrum of silanimine **5d** in hexane at room temperature superimposed with band positions calculated at the TD-B3LYP/6-311+G(d,p) level. Selected calculated transitions: a. assignable to $\pi(\text{Si}=\text{N}) \rightarrow \pi^*(\text{Si}=\text{N})$ transition. b. assignable to $n(\text{N}) \rightarrow \pi^*(\text{Si}=\text{N})$ transition.

and the inversion barrier ΔE_{inv} increase in the same order. As shown in Fig. 9, displaying the relative energy of silanimines **6a–6d** as a function of $\text{Si}-\text{N}-\text{R}$ bending angle θ at the B3LYP/6-311+G(d,p) level, dimethylsilanimines **6a**, **6b** and **6c** have very shallow potential surfaces with respect to bending of the silanimine moiety. A small inversion barrier of silanimines has been already found in $\text{H}_2\text{Si}=\text{NH}_3$ by Schleyer *et al.* (25.1 kJ mol^{-1} at the MP4/6-31G(d) level)¹⁸ and by Gordon (23.4 kJ mol^{-1} at the MP4/MC-611G**//HF/6-31G** level).²⁹ These theoretical calculations show that introduction of a more electropositive group on the nitrogen

Table 2 Absorption maxima and extinction coefficient of silanimines **5a–5d** in hexane at room temperature

Silanimine	$\lambda_{\text{max}}/\text{nm}$ ($\epsilon/(\text{dm}^3 \text{ cm}^{-1} \text{ mol}^{-1})$)		
	Band I ^a	Band II ^b	Band III ^c
5a (R = CH ₂ Ph)	255 (4900)	315 (sh, ^d 150)	—
5b (R = Ph)	251 (9700)	345 (450)	289 (1200)
5c (R = 1-Ad)	246 (6700)	320 (55)	—
5d (R = SiMe ₃)	245 (5400)	306 (30)	—

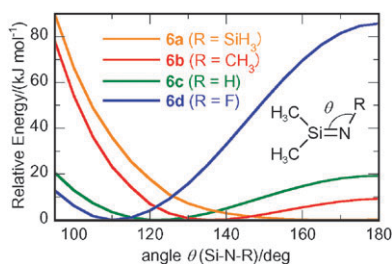
^a Assignable to $\pi(\text{Si}=\text{N}) \rightarrow \pi^*(\text{Si}=\text{N})$ transition. ^b Assignable to $n(\text{N}) \rightarrow \pi^*(\text{Si}=\text{N})$ transition. ^c Assignable to $n(\text{N}) \rightarrow \pi^*(\text{phenyl})$ transition. ^d Shoulder.

atom would increase the p-character of nitrogen lone-pair orbital, resulting in the increase of the Si–N–R bending angle θ (from sp² to sp),³⁰ reduction of the inversion barrier ΔE_{inv} and reduction of the $d(\text{Si}=\text{N})$ value. Similar substituent effects of electropositive groups on the geometry around the C=N double bond in imines have been investigated theoretically.³¹

Since θ and $d(\text{Si}=\text{N})$ of bent silanimines **5a** (138.07(15)°, 1.5823(18) Å) and **5b** (144.42(8)°, 1.5858(9) Å), and almost linear silanimines **5d** (177.19(13)°, 1.5685(18) Å) are in good accord with those calculated for *N*-methylsilanimine **6b** (135.90°, 1.598 Å) and *N*-silylsilanimine **6a** (173.83°, 1.579 Å), respectively, the structural characteristics of silanimines, **5a**, **5b** and **5d** can be explained mainly by the electronic effects of substituents on the dicoordinated nitrogen atom. In contrast, *N*-(1-adamantyl)silanimine **5c** adopts an almost linear structure. The severe steric interaction between the bulky 1-adamantyl substituent and trimethylsilyl group as well as the shallow potentials for bending in silanimines with a carbon functional-group on the nitrogen atom may be responsible for the almost linear structure of silanimine **5c**. Highly symmetric structures of **5a–5d** in solution may be due to the shallow bending potential.

(2) UV-vis spectra. To elucidate the nature of the absorption bands, TD-DFT calculations at the B3LYP/6-311++G(d,p) level were performed for real silanimines **5a–5d**, whose structural parameters were fixed to the experimental values determined by X-ray analysis. The calculated absorption maxima and oscillator strengths of **5a–5d** exhibit good qualitative agreement with the corresponding experimental values of **5a–5d**: the band positions and oscillator strengths for **5a–5d** are superimposed using vertical bars in Fig. 5–8.

Judging from the experimental and theoretical UV-vis spectra, we assigned bands I and II in silanimines **5a–5d** to

**Fig. 9** Relative energies of dimethylsilanimines **6a–6d** as a function of Si–N–R bending angle θ calculated at the B3LYP/6-311 + G(d,p) level.

transitions *a* ($\pi(\text{Si}=\text{N}) \rightarrow \pi^*(\text{Si}=\text{N})$) and *b* ($n(\text{N}) \rightarrow \pi^*(\text{Si}=\text{N})$). The additional weak absorption at 289 nm of **5b** (band III) is assigned as transition *c* ($\pi(\text{phenyl}) \rightarrow \pi^*(\text{Si}=\text{N})$).

Highest occupied, second highest occupied and lowest unoccupied Kohn–Sham orbitals of **5a–5d** calculated at the B3LYP/6-311 + G(d,p) level are the n orbital of nitrogen, and the $\pi(\text{Si}=\text{N})$ and $\pi^*(\text{Si}=\text{N})$ orbitals of silanimine, respectively (Fig. 10). Although the calculated energy levels of the n, $\pi(\text{Si}=\text{N})$ and $\pi^*(\text{Si}=\text{N})$ orbitals are strongly dependent on the substituent on the nitrogen atom, $\pi(\text{Si}=\text{N}) \rightarrow \pi^*(\text{Si}=\text{N})$ transition bands appear at similar wavelength (around 250 nm), probably due to the cancellation of steric and electronic effects of *N*-substituents on the energy levels of $\pi(\text{Si}=\text{N})$ and $\pi^*(\text{Si}=\text{N})$ orbitals. The red-shift of the $n(\text{N}) \rightarrow \pi^*(\text{Si}=\text{N})$ transition band II of *N*-phenylsilanimine **5b** (345 nm) and *N*-1-adamantylsilanimine **5c** (320 nm) compared with those of the other silanimines can be ascribed to the high-lying n orbital resulting from the n– $\pi(\text{aryl})$ interaction being consistent with the perpendicular geometry of silanimine and phenyl rings in **5b**, and resulting from the n– $\sigma(\text{C–C}$ bond in adamantyl moiety) interaction in **5c**, respectively.

(3) Mechanism for formation of silanimines. Although formation of silanimines by the reaction of silylenes with azides have been reported,^{7c,14} the mechanism has not been elucidated. Singlet silylenes have a vacant electrophilic 3p orbital and a nucleophilic n orbital, while azides have nucleophilic and electrophilic nitrogen atoms at 1- and 3-positions, as shown in Scheme 1. In accord with this prediction, the GRRM method that has been developed by Ohno and Maeda¹³ has revealed the following two pathways are the most plausible among possible pathways: (A) electrophilic addition of silylene to the azide followed by elimination of nitrogen molecule, and (B) nucleophilic addition of silylene to the azide followed by elimination of nitrogen molecule, as observed in the reaction of *N*-heterocyclic carbene with azides.^{32,33} Using the GRRM methods, we explored two model reactions: (i) formation of parent silanimine **7a**, H_2Si (**8a**) + HN_3 (**9a**) \rightarrow $\text{H}_2\text{Si}=\text{NH}$ (**7a**) + N_2 (**10**) and (ii) formation of permethylated silanimine **7b**, Me_2Si (**8b**) + MeN_3 (**9b**) \rightarrow $\text{Me}_2\text{Si}=\text{NMe}$ (**7b**) + **10**. The GRRM method enables an automated and systematic reaction route search from an equilibrium structure using anharmonic downward distortion following (ADDF)¹³ and conventional intrinsic reaction coordinate (IRC) following,³⁴ as uphill and downhill methods. The GRRM method has revealed many unknown reaction routes³⁵ and synthetic routes.³⁶

Two reaction routes A and B from **8a** and **9a** to **7a** are predicted at the B3LYP/6-311G(d) level using the GRRM method as shown in Scheme 2. Electrophilic addition of silylene **8a** to azide **9a** gives initial adduct **11a** or **13a** (route A or A'). Adduct **11a** isomerizes to **13a** through the rotation around the Si–N bond with a very low activation energy. Then, elimination of nitrogen molecule from **13a** leads to formation of silanimine **7a**.³⁷ On the other hand, nucleophilic addition of silylene **8a** to azide **9a** gives initial adduct **15** (route B), which undergoes cyclization to give triazasilacyclobutene **17a**. Elimination of nitrogen molecule from **17a** affords silanimine **7a**. Similar two reaction routes for formation of

Table 3 Selected structural parameters and inversion barrier of dimethylsilanimines Me₂Si=NR **6a–6d**^a

Silanimine	$d(\text{Si}=\text{N})/\text{\AA}$	$\theta(\text{Si}-\text{N}-\text{R})/^\circ$ ^b	$\Sigma \varphi(\text{Si})/^\circ$ ^b	$\Delta E_{\text{inv}}/ \text{kJ mol}^{-1}$ ^c
6a (R = SiH ₃)	1.579	173.83	360	0.9
6b (R = CH ₃)	1.598	135.90	360	9.3
6c (R = H)	1.610	120.35	360	19.3
6c (R = H) ^d	1.609	120.5	—	25.1
6d (R = F)	1.656	110.52	360	85.8

^a The geometry was optimized at the B3LYP/6-311+G(d,p) level. ^b Sum of the bond angles around unsaturated silicon atom. ^c $\Delta E_{\text{inv}} = E(\text{linear structure}) - E(\text{optimized bent structure})$. ^d Values from ref. 26. The geometry and energy were calculated at the B3LYP/6-31G(d,p) level.

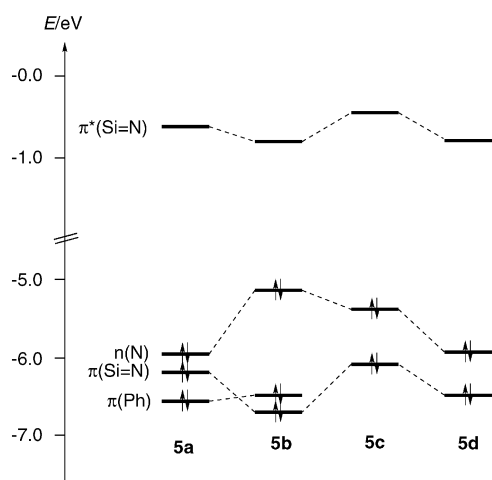
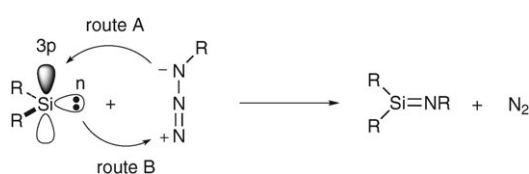


Fig. 10 Frontier Kohn-Sham orbitals (B3LYP/6-311+G(d,p) level) of silanimines **5a–5d** (R^H₂Si=NR) whose structural parameters were set at the experimental values determined by X-ray analysis.

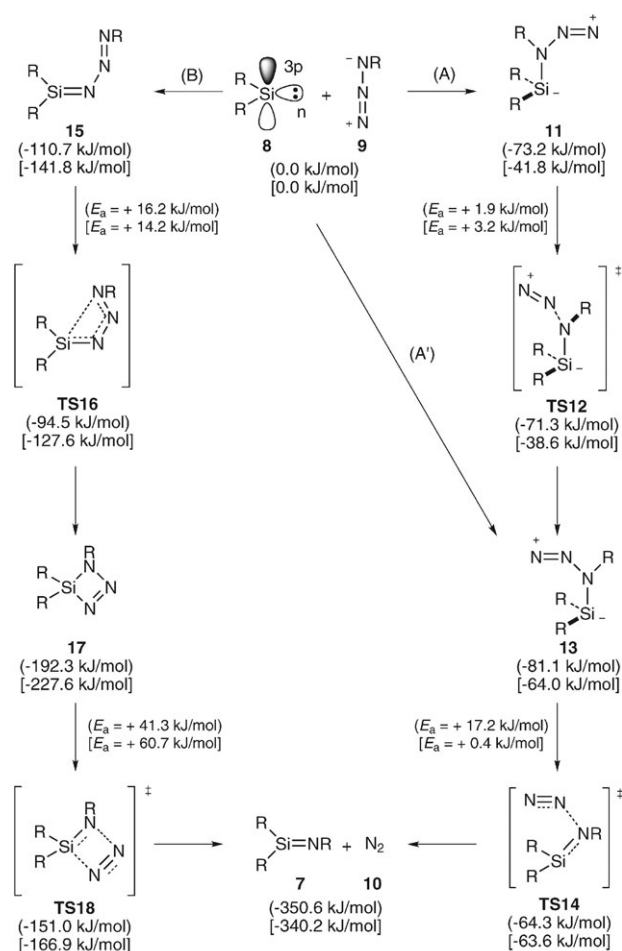


Scheme 1

methylated silanimine **7b** from dimethylsilylene **8b** and methylazide **9b** are predicted at the B3LYP/6-31G(d) level. In both cases (R = H, Me), activation barriers in route A' (or A) are much smaller than those of route B.

Although route A' (or A) is predicted to be favored for the model reactions, the steric congestion around Si–N bond in initial adduct **13** (or **11**) in route A' (or A) is much larger than that in **15** in route B. If the silylene and azide have considerably bulky substituents such as the substituents of silylene **4** and the corresponding azide, initial adduct **13** (or **11**) in route A' (or A) would be destabilized (rather than **15** in route B) owing to the steric congestion, and route A might be less favored.

In the case of reactions of *N*-heterocyclic silylenes and azides reported by Denk and West,^{7e} the corresponding silanimine would form *via* route B because the low-lying 3p orbital for formation of complex **11** is missing in the diaminosilylene owing to the intramolecular interaction of lone pair orbitals of neighboring nitrogen atoms with the 3p orbital of the silylene center.



a, R = H; **b**, R = CH₃

Scheme 2 Possible reaction routes from silylene **8** and azide **9** to the corresponding silanimine **7** and nitrogen molecule (**10**) (**a**: R = H; **b**: R = CH₃). The values of relative energies in kJ mol⁻¹ for R = H calculated at the B3LYP/6-311G(d) level are shown in parentheses and for R = CH₃ calculated at the B3LYP/6-31G(d) level in brackets, respectively.

Conclusions

We successfully synthesized a series of base-free dialkylsilanimines **5a–5d**. Molecular structures determined by X-ray crystallography have shown that **5a–5d** have base-free silicon–nitrogen double bonds, and that bending of the Si=N–R moiety in **5a–5d** is strongly dependent on the electronic and steric effects on the dicoordinated nitrogen atom.

Distinct $\pi(\text{Si}=\text{N}) \rightarrow \pi^*(\text{Si}=\text{N})$ and $n(\text{N}) \rightarrow \pi^*(\text{Si}=\text{N})$ transition bands were observed in the UV-vis spectra. Two plausible mechanisms for formation of silanimine from the reaction of silylene and azide were found using theoretical calculations with the GRRM method for model reactions.

Experimental

General procedures

All reactions were carried out under argon atmosphere using a high-vacuum line, standard Schlenk techniques, a glove box, and dry oxygen-free solvents. ^1H (400 MHz), ^{13}C (100 MHz), and ^{29}Si (79 MHz) NMR spectra were recorded on a Bruker Avance400 spectrometer. Mass spectra were obtained on a JEOL JMS-600W mass spectrometer. UV-vis spectra were recorded on a JASCO V-660 spectrometer. Sampling of air-sensitive compounds were carried out by using a VAC NEXUS 100027 glove box.

Materials

Hexane and benzene- d_6 were dried in a tube covered with a potassium mirror, and then distilled prior to use by using vacuum line. Dialkylsilylene **4**¹¹ and azidobenzene³⁸ were prepared according to the published procedure. (Azidomethyl)benzene, 1-azidoadamantane and azidotrimethylsilane were purchased from commercial sources and used without further purification.

(*N*-Benzyl)dialkylsilanimine **5a**

In a vial equipped with a magnetic stir bar, silylene **4** (42.4 mg, 0.113 mmol) was placed, and then hexane (0.3 ml) was added. To this solution, a hexane solution (1 mL) of (azidomethyl)benzene (15.5 mg, 0.116 mmol) was added dropwise. After stirring the mixture for 5 min, a pale yellow solution was obtained. After hexane was distilled off under the reduced pressure, colorless crystals were obtained. Recrystallization from hexane gave pure (*N*-benzyl)silanimine **5a** (46.9 mg, 0.0981 mmol, 86%) as colorless crystals (Found: C, 57.91; H, 9.71; N, 2.88%. $\text{C}_{23}\text{H}_{47}\text{Si}_5\text{N}$ requires C, 57.79; H, 9.91; N, 2.93); mp 68.1–69.9 °C; $\delta_{\text{H}}(\text{C}_6\text{D}_6, \text{SiMe}_4)$ 0.26 (36 H, s, $\text{Si}(\text{CH}_3)_3$), 1.75 (4 H, s, CH_2), 5.20 (2H, s, CH_2Ph), 7.33 (2H, t, *J* 8, *CH*), 7.65 (2 H, d, *J* 8, *CH*), overlapped with C_6D_6 peak (1H, *CH*); $\delta_{\text{C}}(\text{C}_6\text{D}_6, \text{SiMe}_4)$ 1.75 (SiMe_3), 14.85 (CH_2), 29.42 (C), 52.87 (CH_2Ph), 125.61 (Ph), 127.08 (Ph), 127.92 (Ph), 146.86 (Ph); $\delta_{\text{Si}}(\text{C}_6\text{D}_6, \text{SiMe}_4)$ 2.14 (SiMe_3), 75.34 ($\text{Si}=\text{N}$); $\lambda_{\text{max}}(\text{hexane}, 293 \text{ K})/\text{nm}$ 255 ($\epsilon/\text{dm}^3 \text{ mol}^{-1} \text{ cm}^{-1}$ 4900), 315 (sh, 150); m/z (EI, 30 eV) 477 (21%, M^+), 480 (29), 404 (54).

(*N*-Phenyl)dialkylsilanimine **5b**

According to a procedure similar to the synthesis of **5a**, reaction of silylene **4** (57.6 mg, 0.154 mmol) with azidobenzene (18.5 mg, 0.155 mmol) in hexane (2.0 mL) gave (*N*-phenyl)silanimine **5b** (55.3 mg, 0.119 mmol, 77%) as pale yellow crystals (Found: C, 57.00; H, 9.69; N, 2.99%. $\text{C}_{22}\text{H}_{45}\text{Si}_5\text{N}$ requires C, 56.94; H, 9.77; N, 3.02); mp 103.4–105.4 °C; $\delta_{\text{H}}(\text{C}_6\text{D}_6, \text{SiMe}_4)$ 0.22 (36H, s, SiMe_3), 1.73 (4H, s, CH_2), 6.80 (1H, t, *J* 8.0), 6.92 (2H, d, *J* 8.0), 7.27 (2H, dd, *J* 8.0, 8.0);

$\delta_{\text{C}}(\text{C}_6\text{D}_6, \text{SiMe}_4)$ 1.66, 14.48, 28.97, 117.06, 119.87, 128.81, 150.77; $\delta_{\text{Si}}(\text{C}_6\text{D}_6, \text{SiMe}_4)$ 2.15 (SiMe_3), 59.12 ($\text{Si}=\text{N}$); $\lambda_{\text{max}}(\text{hexane}, 293 \text{ K})/\text{nm}$ 251 ($\epsilon/\text{dm}^3 \text{ mol}^{-1} \text{ cm}^{-1}$ 9700), 289 (1200), 345 (450); m/z (EI, 30 eV) 463 (100%, M^+), 448 (86.7), 390 (16.2).

(*N*-1-Adamantyl)dialkylsilanimine **5c**

According to a procedure similar to the synthesis of **5a**, reaction of silylene **4** (69 mg, 0.19 mmol) with 1-azidoadamantane (29 mg, 0.16 mmol) in hexane (3 mL) gave (*N*-1-adamantyl)silanimine **5c** (74 mg, 0.14 mmol, 88%) as colorless crystals (Found: C, 59.53; H, 10.75; N, 2.74%. $\text{C}_{26}\text{H}_{55}\text{Si}_5\text{N}_1$ requires C, 59.69; H, 10.79; N, 2.68%); mp 218 °C; $\delta_{\text{H}}(\text{C}_6\text{D}_6, \text{SiMe}_4)$ 0.31 (36 H, s, SiMe_3), 1.74 (4H, s, CH_2), 1.63–2.10 (15H, m, adamantyl); $\delta_{\text{C}}(\text{C}_6\text{D}_6, \text{SiMe}_4)$ 2.4 (SiMe_3), 14.3 (C), 29.5 (CH_2), 31.0, 37.3, 50.6 (Adamantyl), 53.5 (C–N); $\delta_{\text{Si}}(\text{C}_6\text{D}_6, \text{SiMe}_4)$ 1.4 (SiMe_3), 19.9 ($\text{Si}=\text{N}$); $\lambda_{\text{max}}(\text{hexane}, 293 \text{ K})/\text{nm}$ 246 ($\epsilon/\text{dm}^3 \text{ mol}^{-1} \text{ cm}^{-1}$ 6700), 320 (55); m/z (EI, 70 eV) 521 (13%, M^+), 463 (26), 135 (95), 73 (100).

(*N*-Trimethylsilyl)dialkylsilanimine **5d**

According to a procedure similar to the synthesis of **5a**, reaction of silylene **4** (62 mg, 0.17 mmol) with azidotrimethylsilane (20 mg, 0.17 mmol) in hexane (3 mL) gave (*N*-trimethylsilyl)silanimine **5d** (65 mg, 0.14 mmol, 82%) as colorless crystals (Found: C, 49.22; H, 10.50; N, 2.84. $\text{C}_{19}\text{H}_{49}\text{Si}_6\text{N}_1$ requires C, 49.59; H, 10.73; N, 3.05); mp 139 °C; $\delta_{\text{H}}(\text{C}_6\text{D}_6, \text{SiMe}_4)$ 0.24 (36 H, s, SiMe_3), 0.36 (9H, s, *N*- SiMe_3), 1.72 (s, 4 H, CH_2); $\delta_{\text{C}}(\text{C}_6\text{D}_6, \text{SiMe}_4)$ 2.0 (SiMe_3), 4.5 (SiMe_3), 17.1(C), 29.5 (CH_2); $\delta_{\text{Si}}(\text{C}_6\text{D}_6, \text{SiMe}_4)$ –15.50 (*N*- SiMe_3), 1.4 (SiMe_3), 89.9 ($\text{Si}=\text{N}$); $\lambda_{\text{max}}(\text{hexane}, 293 \text{ K})/\text{nm}$ 218 ($\epsilon/\text{dm}^3 \text{ mol}^{-1} \text{ cm}^{-1}$ 6300), 245 (5400), 306 (30); m/z (EI, 70 eV) 461 (12%, M^+), 275 (21), 231 (28), 73 (100).

Crystal structure determination of silanimines

Single crystals of silanimines **5a–5d** suitable for X-ray diffraction study were obtained by recrystallization from hexane. A single crystal of **5a–5d** coated with apiezon grease was mounted on a thin glass fiber and transferred to the cold gas stream of the diffractometer. X-ray diffraction data were collected on a BrukerAXS APEXII diffractometer with graphite-monochromated Mo-K α radiation (λ 0.71073 Å). The data were corrected for Lorentz and polarization effects. An empirical absorption correction based on the multiple measurement of equivalent reflections was applied using the program SADABS.³⁹ The structures were solved by direct methods and refined by full-matrix least-squares against F^2 using all data (SHELXL-97).⁴⁰

Crystal data for 5a. $\text{C}_{23}\text{H}_{47}\text{NSi}_5$, $M = 478.07$, triclinic, $a = 10.844(2)$, $b = 11.874(3)$, $c = 13.349(3)$ Å, $\alpha = 115.304(2)$, $\beta = 95.635(2)$, $\gamma = 107.048(2)^\circ$, $V = 1435.1(5)$ Å³, $T = 100 \text{ K}$, space group $P\bar{1}$ (no. 2), $Z = 2$, 13 815 reflections measured, 5027 unique ($R_{\text{int}} = 0.0340$) which were used in all calculations. The final R_1 and $wR(F^2)$ were 0.0375 ($I > 2\sigma(I)$) and 0.0975 (all data).

Crystal data for 5b. C₂₂H₄₅NSi₅, $M = 464.04$, monoclinic, $a = 9.1616(9)$, $b = 20.601(2)$, $c = 14.7242(14)$ Å, $\beta = 93.9340(10)^\circ$, $V = 2772.5(5)$ Å³, $T = 100$ K, space group $P2_1/n$ (no. 14), $Z = 4$, 31 160 reflections measured, 6256 unique ($R_{\text{int}} = 0.0280$) which were used in all calculations. The final R_1 and $wR(F^2)$ were 0.0250 ($I > 2\sigma(I)$) and 0.0719 (all data).

Crystal data for 5c. C₂₆H₅₅NSi₅, $M = 522.16$, triclinic, $a = 9.445(3)$, $b = 10.618(3)$, $c = 16.947(5)$ Å, $\alpha = 95.035(3)$, $\beta = 93.948(3)$, $\gamma = 111.147(3)^\circ$, $V = 1569.7(8)$ Å³, $T = 120$ K, space group $P\bar{1}$ (no. 2), $Z = 2$, 17 268 reflections measured, 6926 unique ($R_{\text{int}} = 0.0280$) which were used in all calculations. The final R_1 and $wR(F^2)$ were 0.0381 ($I > 2\sigma(I)$) and 0.1064 (all data).

Crystal data for 5d. C₁₉H₄₉NSi₆, $M = 460.13$, monoclinic, $a = 14.673(5)$, $b = 9.188(3)$, $c = 21.868(8)$ Å, $\beta = 96.864(4)^\circ$, $V = 2927.0(17)$ Å³, $T = 120$ K, space group $P2_1/c$ (no. 14), $Z = 2$, 25 067 reflections measured, 6344 unique ($R_{\text{int}} = 0.0531$) which were used in all calculations. The final R_1 and $wR(F^2)$ were 0.0415 ($I > 2\sigma(I)$) and 0.1145 (all data).

Theoretical calculations

All theoretical calculations were performed using a Gaussian 03⁴¹ program and reaction routes were searched by the ADDF¹³ and IRC³⁴ methods available in the GRRM 1.2 program.¹³ Geometry optimization and potential surface search of **6a–6d** as a function of Si–N–R bending angle θ for model compounds was carried out at the B3LYP/6-311+G(d,p) level. Optimized atomic coordinates of **6a–6d** are summarized in the ESI†. Absorption band maxima and oscillator strengths of **5a–5d** (whose structural parameters were fixed to the experimental values determined by X-ray analysis) were calculated at the TD-B3LYP/6-311+G(d,p) level. For a reaction route search for formation of silanimines H₂Si=NH (**7a**), initial adducts **11a** and **15a** (whose geometries were optimized at the B3LYP/6-311G(d) level) were used as initial structures for the GRRM method.¹³ For exploration of low-barrier routes to **7a**, the large-ADD (*l*ADD) method was applied.^{13d} Although automatic reaction route search using GRRM methods explored various reaction routes among H₃SiN isomers including **7a**, only the reaction routes to **7a** with the smallest activation barrier, except for the degenerate rearrangements such as a configuration inversion, are shown in Fig. 10. For a reaction route search for formation of silanimines Me₂Si=NMe (**7b**), the corresponding equilibrium structures (EQ) and transition state structures (TS) **7b–TS18b** were optimized at the B3LYP/6-31G(d) level. Optimized atomic coordinates of **7**, and **11–TS18** are also summarized in the ESI.

Acknowledgements

This work was supported by the Ministry of Education, Culture, Sports, Science, and Technology of Japan [Specially Promoted Research (No. 17002005, M.K. and T.I.), a Grant-in-Aid for Scientific Research on Innovative Areas (No. 21108501, “pi-Space”, T.I.), and a Grant-in-Aid for Scientific Research B (No. 21350007, T.I. and K.O.)].

References

- 1 A. G. Brook, F. Abdesaken, B. Gutekunst, A. Gutekunst and R. K. Kallury, *J. Chem. Soc., Chem. Commun.*, 1981, 191.
- 2 R. West, M. J. Fink and J. Michl, *Science*, 1981, **214**, 1343.
- 3 For reviews of silanimines, see: I. Hemme and U. Klingebiel, *Adv. Organomet. Chem.*, 1996, **39**, 159; T. Müller, W. Ziche, and N. Auner, in *The Chemistry of Organic Silicon Compounds*, ed. Z. Rappoport and Y. Apeloig, John Wiley & Sons, New York, 1998, vol. 2, ch. 16, p. 857; P. Neugebauer, B. Jaschke and U. Klingebiel, ed. Z. Rappoport and Y. Apeloig, John Wiley & Sons, New York, 2001, ch. 6, p. 429; U. Klingebiel and C. Matthes, *J. Organomet. Chem.*, 2007, **692**, 2633.
- 4 N. Wiberg, S. Schurz and G. Fischer, *Angew. Chem., Int. Ed. Engl.*, 1986, **24**, 1053.
- 5 N. Wiberg, K. Schurz, G. Reber and G. Müller, *J. Chem. Soc., Chem. Commun.*, 1985, 591.
- 6 M. Hasse and U. Klingebiel, *Angew. Chem., Int. Ed. Engl.*, 1986, **25**, 649.
- 7 For examples of synthesis of Lewis base-coordinated silanimines, see: (a) N. Wiberg, K. Schurz, G. Müller and J. Riede, *Angew. Chem., Int. Ed. Engl.*, 1988, **27**, 935; (b) N. Wiberg and K. Schurz, *J. Organomet. Chem.*, 1988, **341**, 145; (c) G. Reber, J. Riede, N. Wiberg, K. Schurz and G. Müller, *Z. Naturforsch. B*, 1989, **44**, 786; (d) S. Walter, U. Klingebiel and D. Schmidt-Base, *J. Organomet. Chem.*, 1991, **412**, 319; (e) M. Denk, R. K. Hayashi and R. West, *J. Am. Chem. Soc.*, 1994, **116**, 10813; (f) K. Junge, E. Popowski and M. Michalik, *Z. Anorg. Allg. Chem.*, 1999, **625**, 1532; (g) H.-W. Lerner, N. Wiberg and J. W. Bats, *J. Organomet. Chem.*, 2005, **690**, 3898; (h) H.-W. Lerner, M. Bolte, K. Schurz, N. Wiberg, G. Baum, D. Fenske, J. W. Bats and M. Wagner, *Eur. J. Inorg. Chem.*, 2006, 4998.
- 8 For examples of synthesis of metal halides-coordinated silanimines, see: (a) R. Boese and U. Klingebiel, *J. Organomet. Chem.*, 1986, **315**, C17; (b) D. Stalke, U. Pieper, S. Vollbrecht and U. Klingebiel, *Z. Naturforsch. B*, 1990, **45**, 1513; (c) D. Grosskopf, L. Marcus, U. Klingebiel and M. Noltemeyer, *Phosphorus, Sulfur Silicon Relat. Elem.*, 1994, **97**, 113; (d) M. Jendras, U. Klingebiel and M. Noltemeyer, *J. Organomet. Chem.*, 2002, **646**, 134.
- 9 L. J. Procopio, P. J. Carroll and D. H. Berry, *J. Am. Chem. Soc.*, 1991, **113**, 1870; L. J. Procopio, P. J. Carroll and D. H. Berry, *Polyhedron*, 1995, **14**, 45.
- 10 J. Niesmann, U. Klingebiel, M. Schafer and R. Boese, *Organometallics*, 1998, **17**, 947.
- 11 M. Kira, T. Iwamoto, C. Kabuto and S. Ishida, *J. Am. Chem. Soc.*, 1999, **121**, 9722. For a recent review of the chemistry of silylene **4**, see: M. Kira, T. Iwamoto and S. Ishida, *Bull. Chem. Soc. Jpn.*, 2007, **80**, 258.
- 12 For our recent studies on the unsaturated silicon compounds with alkylsubstituents, see: (a) S. Ishida, T. Iwamoto, C. Kabuto and M. Kira, *Nature*, 2003, **421**, 725; (b) T. Iwamoto, T. Abe, C. Kabuto and M. Kira, *Chem. Commun.*, 2005, 5190; (c) T. Iwamoto, K. Sato, S. Ishida, C. Kabuto and M. Kira, *J. Am. Chem. Soc.*, 2006, **128**, 16914; (d) T. Abe, T. Iwamoto, C. Kabuto and M. Kira, *J. Am. Chem. Soc.*, 2006, **128**, 4228; (e) R. Tanaka, T. Iwamoto and M. Kira, *Angew. Chem., Int. Ed.*, 2006, **45**, 6371; (f) K. Uchiyama, S. Nagendran, S. Ishida, T. Iwamoto and M. Kira, *J. Am. Chem. Soc.*, 2007, **129**, 10638; (g) T. Iwamoto, M. Kobayashi, K. Uchiyama, S. Sasaki, S. Nagendran, H. Isobe and M. Kira, *J. Am. Chem. Soc.*, 2009, **131**, 3156. See, also C. Watanabe, T. Iwamoto, C. Kabuto and M. Kira, *Angew. Chem., Int. Ed.*, 2008, **47**, 5386.
- 13 (a) K. Ohno and S. Maeda, *Chem. Phys. Lett.*, 2004, **384**, 277; (b) S. Maeda and K. Ohno, *J. Phys. Chem. A*, 2005, **109**, 5742; (c) K. Ohno and S. Maeda, *J. Phys. Chem. A*, 2006, **110**, 8933; (d) S. Maeda and K. Ohno, *J. Phys. Chem. A*, 2007, **111**, 4527.
- 14 For reactions of silylenes with azides, see: M. Weidenbruch, B. Brand-Roth, S. Pohl and W. Saak, *J. Organomet. Chem.*, 1989, **379**, 217. See also ref. 7e.
- 15 Reaction proceeded even at -60 °C.
- 16 (a) R. West and M. Denk, *Pure Appl. Chem.*, 1996, **68**, 785; (b) B. Gehrhus, P. B. Hitchcock and M. F. Lappert, *Z. Anorg. Allg. Chem.*, 2001, **627**, 1048; (c) N. J. Hill, D. F. Moser, I. Guzei and R. West, *Organometallics*, 2005, **24**, 3346; (d) A. C. Tomasic,

- A. Mitra and R. West, *Organometallics*, 2009, **28**, 378; (e) Y. Xiong, S. Yao and M. Driess, *Chem. Eur. J.*, 2009, **15**, 8542.
- 17 M. Kaftory, M. Kapon and M. Botshansky, in *Chemistry of Organic Silicon Compounds*, ed. Y. Apeloig and Z. Rappoport, John Wiley & Sons, New York, 1998, vol. 2, ch. 5, pp. 181–265.
- 18 P. v. R. Schleyer and P. D. Stout, *J. Chem. Soc., Chem. Commun.*, 1986, 1373.
- 19 H.-W. Lerner, M. Bolte, K. Schurz, N. Wiberg, G. Baum, D. Fenske, J. W. Bats and M. Wagner, *Chem. Eur. J.*, 2006, 4998.
- 20 P. A. Tucker, A. Hoekstra, J. M. Ten Cate and A. Vos, *Acta Crystallogr., Sect. B: Struct. Crystallogr. Cryst. Chem.*, 1975, **31**, 733.
- 21 D.-J. Wang, L. Fan and G.-H. Wang, *Z. Kristallogr., New Chem. Struct.*, 2009, **224**, 186.
- 22 A plot of δSi_u of **6b** as a function of the Si–N–R bending angle θ is shown in the ESI†.
- 23 S. S. Zigler, K. M. Welsh and R. West, *J. Am. Chem. Soc.*, 1987, **109**, 4392.
- 24 S. S. Zigler, L. M. Johnson and R. West, *J. Organomet. Chem.*, 1988, **341**, 187.
- 25 J. G. Radziszewski, P. Kaszynski, D. Littmann, V. Balaji, B. A. Hess, Jr. and J. Michl, *J. Am. Chem. Soc.*, 1993, **115**, 8401.
- 26 A. Kuhn and W. Sander, *Organometallics*, 1998, **17**, 4776.
- 27 A. Sekiguchi, W. Ando and K. Honda, *Chem. Lett.*, 1985, 1029.
- 28 Sander *et al.* have shown that substituents on the silicon atoms of silanimines are predicted to affect the geometry around the Si=N bond. See ref. 26.
- 29 T. N. Truong and M. S. Gordon, *J. Am. Chem. Soc.*, 1986, **108**, 1775.
- 30 H. A. Bent, *Chem. Rev.*, 1961, **61**, 275.
- 31 M. A. McAllister and T. T. Tidwell, *J. Chem. Soc., Perkin Trans. 2*, 1994, 2239. For the substituent effects on the inversion barrier in imines, see also: J. Gálvez and A. Guirado, *J. Comput. Chem.*, 2010, **31**, 520; J.-M. Lehn, *Chem. Eur. J.*, 2006, **12**, 5910, and references cited therein.
- 32 Formation of triazene from NHC with azide: (a) M. Tamm, S. Randoll, T. Bannenberg and E. Herdtweck, *Chem. Commun.*, 2004, 876; (b) D. M. Khramov and C. W. Bielawski, *Chem. Commun.*, 2005, 4958; (c) D. M. Khramov and C. W. Bielawski, *J. Org. Chem.*, 2007, **72**, 9407; (d) M. Tamm, D. Petrovic, S. Randoll, S. Beer, T. Bannenberg, P. G. Jones and J. Grunenberg, *Org. Biomol. Chem.*, 2007, **5**, 523; (e) D. J. Coady, D. M. Khramov, B. C. Norris, A. G. Tennyson and C. W. Bielawski, *Angew. Chem., Int. Ed.*, 2009, **48**, 5187.
- 33 Formation of imine from NHC with trimethylsilylazide: J. M. Hopkins, M. Bowdridge, K. N. Robertson, T. S. Cameron, H. A. Jenkins and J. A. C. Clyburne, *J. Org. Chem.*, 2001, **66**, 5713.
- 34 (a) K. Fukui, *Acc. Chem. Res.*, 1981, **14**, 363; (b) K. Ishida, K. Morokuma and A. Komornicki, *J. Chem. Phys.*, 1977, **66**, 2153; (c) M. Page and J. W. McIver, *J. Chem. Phys.*, 1988, **88**, 922; (d) C. Gonzalez and H. B. Schlegel, *J. Chem. Phys.*, 1989, **90**, 2154.
- 35 (a) X. Yang, S. Maeda and K. Ohno, *J. Phys. Chem. A*, 2005, **109**, 7319; (b) X. Yang, S. Maeda and K. Ohno, *Chem. Phys. Lett.*, 2006, **418**, 208; (c) X. Yang, S. Maeda and K. Ohno, *J. Phys. Chem. A*, 2007, **111**, 5099; (d) Y. Watanabe, S. Maeda and K. Ohno, *Chem. Phys. Lett.*, 2007, **447**, 21; (e) S. Maeda and K. Ohno, *Chem. Phys. Lett.*, 2008, **460**, 55; (f) K. Ohno and S. Maeda, *Phys. Scr.*, 2008, **78**, 058122; (g) M. Moteki, S. Maeda and K. Ohno, *Organometallics*, 2009, **28**, 2218; (h) S. Maeda K. Ohno and K. Morokuma, *J. Chem. Theory Comput.*, 2009, **5**, 2734.
- 36 The GRRM method can find a dissociation channel (DC) from an equilibrium structure (EQ) to its fragments. The reverse route of DC can be regarded as a synthetic route to the EQ from the fragments: (a) S. Maeda and K. Ohno, *Chem. Lett.*, 2004, **33**, 1372; (b) S. Maeda and K. Ohno, *Chem. Phys. Lett.*, 2004, **398**, 240; (c) S. Maeda and K. Ohno, *Astrophys. J.*, 2006, **640**, 823.
- 37 Facile elimination of a nitrogen molecule from **13** compared with **11** may be owing to the geometry around the Si–N moiety, where the lone-pair on the silicon atom and the σ^* orbital of (N₂)–N bond are antiperiplanar to each other, effectively stabilizing the transition state for elimination of the nitrogen molecule.
- 38 A. Cxikilicki and K. Rehse, *Arch. Pharm.*, 2004, **337**, 156.
- 39 G. M. Sheldrick, *SADABS, Empirical Absorption Correction Program*, Göttingen, Germany, 1996.
- 40 G. M. Sheldrick, *SHELXL-97, Program for the Refinement of Crystal Structures*, University of Göttingen, Germany, 1997.
- 41 M. J. Frisch, G. W. Trucks, H. B. Schlegel, G. E. Scuseria, M. A. Robb, J. R. Cheeseman, J. A. Montgomery, Jr., T. Vreven, K. N. Kudin, J. C. Burant, J. M. Millam, S. S. Iyengar, J. Tomasi, V. Barone, B. Mennucci, M. Cossi, G. Scalmani, N. Rega, G. A. Petersson, H. Nakatsuji, M. Hada, M. Ehara, K. Toyota, R. Fukuda, J. Hasegawa, M. Ishida, T. Nakajima, Y. Honda, O. Kitao, H. Nakai, M. Klene, X. Li, J. E. Knox, H. P. Hratchian, J. B. Cross, V. Bakken, C. Adamo, J. Jaramillo, R. Gomperts, R. E. Stratmann, O. Yazyev, A. J. Austin, R. Cammi, C. Pomelli, J. W. Ochterski, P. Y. Ayala, K. Morokuma, G. A. Voth, P. Salvador, J. J. Dannenberg, V. G. Zakrzewski, S. Dapprich, A. D. Daniels, M. C. Strain, O. Farkas, D. K. Malick, A. D. Rabuck, K. Raghavachari, J. B. Foresman, J. V. Ortiz, Q. Cui, A. G. Baboul, S. Clifford, J. Cioslowski, B. B. Stefanov, G. Liu, A. Liashenko, P. Piskorz, I. Komaromi, R. L. Martin, D. J. Fox, T. Keith, M. A. Al-Laham, C. Y. Peng, A. Nanayakkara, M. Challacombe, P. M. W. Gill, B. Johnson, W. Chen, M. W. Wong, C. Gonzalez and J. A. Pople, *GAUSSIAN 03, Revision E.01*, Gaussian, Inc., Wallingford CT, 2004.